JOURNAL OF Applied Polymer SCIENCE

Preparation and Properties of Multiwalled Carbon Nanotube/ Epoxy-Amine Composites

P. Jyotishkumar,[1] Emmanuel Logakis,[2] Sajeev Martin George,[1] Jürgen Pionteck,[3] Liane Häussler,[3] Rüdiger Haßler,[3] Polycarpos Pissis,[2] Sabu Thomas[1,4,5,6]

[1]School of Chemical Sciences, Mahatma Gandhi University, Priyadarshini Hills, Kottayam, Kerala 686560, India
[2]Department of Physics, National Technical University of Athens, Zografou Campus, 15780 Athens, Greece
[3]Department of Polymer Reactions and Blends, Leibniz Institute of Polymer Research Dresden, 01069 Dresden, Germany
[4]Centre for Nanoscience and Nanotechnology, Mahatma Gandhi University, Priyadarshini Hills, Kottayam, Kerala 686560, India
[5]Faculty of Applied Sciences, Universiti Teknologi MARA, 40450 Shah Alam, Selongor, Malaysia
[6]Center of Excellence for Polymer Materials and Technologies, Tehnoloski Park 24, 1000 Ljubljana, Slovenia
Correspondence to: P. Jyotishkumar (E-mail: jyotishkumarp@gmail.com) or S. Thomas (E-mail: sabupolymer@yahoo.com)

ABSTRACT: Different amounts of multiwalled carbon tubes (MWCNTs) were incorporated into an epoxy resin based on diglycidyl ether of bisphenol A and both epoxy precursor and composite were cured with 4,4′-diamino diphenyl sulfone. Transmission and scanning electron microscopy demonstrated that the carbon nanotubes are dispersed well in the epoxy matrix. Differential scanning calorimetry measurements confirmed the decrease in overall cure by the addition of MWCNTs. A decrease in volume shrinkage of the epoxy matrix caused by the addition of MWCNTs was observed by pressure–volume–temperature measurements. Thermomechanical and dynamic mechanical analysis were performed for the MWCNT/epoxy composites, showing that the T_g was slightly affected, whereas the dimensional stability and stiffness are improved by the addition of MWCNTs. Electrical conductivity measurements of the composite samples showed that an insulator to conductor transition takes place between 0.019 and 0.037 wt % MWCNTs. The addition of MWCNTs induces an increase in both impact strength (18%) and fracture toughness (38%) of the epoxy matrix with very low filler content. © 2012 Wiley Periodicals, Inc. J. Appl. Polym. Sci. 000: 000–000, 2012

KEYWORDS: epoxy composites; volume shrinkage; thermal properties; impact strength; fracture toughness

Received 3 October 2011; accepted 25 February 2012; published online
DOI: 10.1002/app.37674

INTRODUCTION

The development of new materials with advanced properties has created a new era in the application field. The discovery of carbon nanotubes (CNTs) and carbon nanostructured materials has inspired scientists to develop materials for a range of potential applications.[1,2] Nanoengineered materials such as carbon nanotubes and fibers, with their outstanding characteristic features, hold a key position for the development and use of super-performing composites for several advanced applications.[3] CNTs are excellent candidates for multifunctional nanoreinforcing for a variety of polymers, ceramics, and metals. Because of their high aspect ratio, low density, and their exceptional physical properties (electrical, thermal, and mechanical), composites based on CNTs have attracted great interest.[4–8] CNTs have been already employed for devices ranging from golf clubs, military aircrafts, scanning electron microscopy tips, microelectronic devices, etc.[3]

Different polymer composites have been synthesized by incorporating MWCNTs into various polymer matrices, such as polyamides, polyimides, epoxy resins, polyurethane, and polypropylene. Previous results indicated that the addition of small amounts of MWCNTs, less than 1 wt %, can significantly improve the thermal, mechanical, and electrical properties without compromising the processability of the host polymer.[6,9,10] These polymer composites gain their high properties, particularly mechanical properties, at low filler content owning to the high aspect ratio and high surface area to volume ratio of the MWCNTs.

Epoxy resins are widely used in industrial applications, as construction materials, in automobile industry, aerospace applications, as adhesives, coatings, electronic circuit board laminates etc., due to their good stiffness, dimensional stability, good chemical and water resistance, low cost, ease of processing, fine

adhesion to many substrates, low specific weight, low shrinkage on cure, and long pot life period. Toughness reinforcement of epoxy resins has attracted considerable attention over the last 30 years.[11–14] Many recent investigations are focused on further improvement of epoxy materials using nanofillers and particularly with MWCNTs. Extensive work that has been dedicated to this topic over the last decade[15–23]; however, a few reports indicate that MWCNTs reinforced epoxy composites were weaker or only slightly stronger than the neat crosslinked epoxy. For instance, Lau et al. found that the use of MWCNTs for advanced composite structures not improve the structural mechanical strength of the epoxy composites.[24] On the other hand, there was large number of reports showing a significant improvement in thermal and mechanical properties of MWCNTs-modified epoxy systems.[25–27] These studies revealed the importance of good dispersion as well as interpenetration of MWCNTs with epoxy resins is very important for the improvement in properties.

The tendency of polymers to expand or contract during processing is a problem that has been widely recognized, especially for epoxy composites. Being cured in geometrically constrained environment cure shrinkage generates large residual stresses that further lead to severe manufacturing and application problems of the epoxy based materials. Thus, the knowledge of volume shrinkage behavior during curing of the epoxy resin system is particularly necessary to have a correct control of the processing mechanism and the subsequent engineering design. In spite of few works that has been dedicated to this topic,[28] no attempt has been made to understand the effect of MWCNTs on epoxy volume shrinkage by pressure–volume–temperature (PVT) measurements; in this context, a detailed study is necessary.

In this article, we present a study on preparation and properties of epoxy-amine composites with small quantities of MWCNTs. The curing shrinkage, thermal, mechanical, electrical, and morphological properties of MWCNT/epoxy composites were investigated as a function of filler content. The relationship between morphology and the thermomechanical properties of MWCNT/epoxy composites was explored. In addition, toughening mechanism was investigated in detail. The resulting composites were found to have improved toughness retaining at the same time the thermomechanical properties of the neat epoxy system and exhibit high electrical conductivity above the very low percolation concentration of $\leq$0.037 wt % MWCNTs.

EXPERIMENTAL

Materials

The epoxy resin, diglycidyl ether of bisphenol-A (DGEBA) (Lapox L-12, Atul, India) was used as matrix. The glass transition temperature of the epoxy resin is –20°C, as was obtained from differential scanning calorimetry (DSC) measurements. The amine hardener 4,4′-diamino diphenyl sulfone (DDS) (Lapox K-10, Atul, India.) was used as a cross linker for epoxy. The used MWCNTs (Baytube® 150P) was supplied from Bayer Material Science AG (Leverkusen, Germany) synthesized by catalytic carbon vapor disposition process (purity $>$ 95%, average diameter 13–16 nm, length $>$ 1 μm).

Composite Preparation

Different amount of MWCNTs were dispersed in 100 g epoxy using a sonicator for 15 min. In a second step 35 g DDS was added to the MWCNT/epoxy monomer mixture with an stoichiometric epoxy:amine ratio of 2:1. After dissolving the DDS in epoxy resin, the composites were cured in an open mould at 180°C for 3 h and then post curing at 200°C for 2 h. The samples were named according to the final MWCNTs concentration as 0.007 wt % MWCNTs, 0.019 wt % MWCNTs, 0.037 wt % MWCNTs, 0.056 wt % MWCNTs, 0.074 wt % MWCNTs, 0.22 wt % MWCNTs, 0.37 wt % MWCNTs, and 0.74 wt % MWCNTs. (*For comparison, a sample without MWCNTs was prepared, named as neat epoxy).

For differential scanning calorimetry (DSC) and PVT observations, the freshly prepared mixtures were immediately used or stored before use in a freezer at −20°C. For other experiments, the freshly prepared mixtures were cured in the air oven at 180°C for 3 h and then post-cured at 200°C for further 2 h. The resultant composites were then allowed to cool slowly to room temperature.

CHARACTERIZATION

Transmission Electron Microscopy

TEM observations were carried out using a high-resolution transmission electron microscope JEM – 2100 HR-TEM (JEOL, Japan) with an accelerating voltage of 200 kV to examine the morphology as well as the state of dispersion of MWCNTs. Samples were cut into 50 to 80 nm thick films by ultra microtome. For the observation of the nanopowders, MWCNTs were dispersed in ethanol under sonication for 10 minutes. Then the suspension was dropped on a copper grid and analyzed by HR-TEM.

Field Emission Scanning Electron Microscopy

The morphology of fractured surface of crosslinked epoxy composites was examined using an ULTRA FESEM (model ULTRA plus, Carl Zeiss NTS GmbH, Germany). The samples were coated with platinum by vapor deposition using a SCD 500 Sputter Coater (BAL-TEC AG, Lichtenstein).

Differential Scanning Calorimetry

The non-cured samples were analyzed using a DSC Q1000 of TA-Instruments. Samples of about 6 mg were encapsulated in aluminum pans. Modulated DSC measurements were carried out in the temperature range from −60°C (5 min.) to 300°C (0.5 min.) at a heating rate of 2 K/min. in N_2 atmosphere with an amplitude of +/− 0.31 K and a period of 40 s. The cooling was done at 40 K/min. without modulation, before heating again with the same conditions as in the first heating run to analyze the completeness of curing. It is important to add that at higher heating rates the curing reaction was not complete up to 300°C. Above this temperature, the beginning of degradation process (proven by thermogravimetric analyses (TGA), which are not shown here) overlaps with the curing reaction. Thus, to ensure complete curing below 300°C the low heating rate had to be used in this work. The heat of the reaction (ΔH) was determined from the total heat flow of the first heating scan. The curing enthalpy is proportional to the extent of the

reaction. In the composites, the measured curing enthalpy ΔH is normalized with respect to the epoxy content ($\Delta H_{(corr)}$).

Pressure–Volume–Temperature Analysis

The PVT measurements were done using a fully automated GNOMIX high-pressure mercury dilatometer. Below 200°C, the absolute accuracy of the instrument is of 0.002 cm^3/g. In practice, changes in specific volume as small as 0.0002 cm^3/g can be resolved reliably. The crosslinking reaction was characterized in the so called data acquisition mode (DAQ) at 10 MPa and 180°C following the volume shrinkage of the samples as a function of time (13 h). To check whether any crosslinking has taken place during the sample preparation stages, the experimental initial specific volumes were compared with those calculated from the value of the individual components by assuming an additive behavior (Table I). The experimental specific volumes and calculated specific volumes are comparable, the deviation was within an acceptable range (1%). This means that no curing or only little curing takes place during sampling.

Dynamic Mechanical Analysis

The investigation of the thermomechanical properties was performed using dynamic mechanical analysis (DMA 2980, TA instruments). Rectangular specimens of 40 × 10 × 3 mm^3 were used. The analysis was done in single cantilever mode at a frequency of 1 Hz, in the temperature range from −100 to 300°C and at a heating rate of 1 K/min.

Thermomechanical Analysis

The thermomechanical properties of neat epoxy and MWCNT/epoxy composites were measured using a TA instrument Q400 thermomechanical analyzer. The samples were scanned from 50 to 250°C at a heating rate of 1 K/min. Rectangular specimens of 20 × 10 × 3 mm^3 were used for the analysis.

Dielectric Relaxation Spectroscopy

The electrical properties of the prepared materials were studied by employing dielectric relaxation spectroscopy. In this technique, the sample is placed between the plates of a capacitor, an alternate voltage is applied, and the response of the system is studied. By measuring the complex impedance ($Z^* = Z' - iZ''$) of the circuit the complex permittivity ($\varepsilon^* = \varepsilon' - i\varepsilon''$) arises from the following equation:

$$\varepsilon^*(\omega) = \frac{1}{i\omega Z^*(\omega) C_0} \tag{1}$$

where ω is the angular frequency ($\omega = 2\pi f$) of the applied electric field and C_0 the equivalent capacitance of the empty capacitor. The frequency-dependent ac conductivity (real part, σ') is then obtained from the following equation:

$$\sigma'(\omega) = \varepsilon_0 \omega \varepsilon''(\omega) \tag{2}$$

where $\varepsilon_0 = 8.85 \times 10^{-12}$ F m^{-1} is the permittivity of free space. In this work, DRS measurements at room temperature were carried out in a wide frequency range of 10^{-2} to 10^6 Hz by means of a Novocontrol Alpha analyzer (Germany).

Impact Strength

Charpy impact strength of the unmodified and modified epoxy resin was measured following the specifications ISO 179/1eA.

Table I. Experimental and Calculated Initial Specific Volume for Epoxy DDS System and 0.37 wt % MWCNTs Containing Composites at 180°C

Samples	Specific volume (experimental) cm^3/g V_{sp,E_0}	Specific volume (calculated) cm^3/g V_{sp,T_0}
Neat epoxy	0.893	0.900
0.37 wt % MWCNTs	0.901	0.898

Impact tests were performed on Zorn Stendal impact testing machine. The dimensions of the specimens were approximately 40 × 8 × 4 mm^3.

Fracture Toughness

Fracture toughness of the specimens was determined according to ASTM D 5045-99. The measurements were taken with a universal testing machine Zwick (UPM - Z010). The material is taken in the form of rectangular sheet, the specimen thickness, d = 4 mm, was taken and it is identical with the sheet thickness. The sample width, b equals $2d$. In the specimen geometry the crack length, a, is selected in such a way that $0.45 < a/d < 0.55$. The analysis was done in bending mode at room temperature. The value of stress intensity factor (K_{IC}) was calculated using Eq. (3).

$$K_{IC} = QPa^{1/2}/bd \tag{3}$$

where P is the load at the initiation of crack, a is the crack length, b is the width of the specimen, d is the thickness of the specimen, and Q is geometry constant$Q$ is calculated using the following equation[29]:

$$Q = 1.99 - 0.41(a/b) + 18.7(a/b)^2 - 38.48(a/b)^3 + 53.85(a/b)^4 \tag{4}$$

RESULTS

Electron Microscopy

The TEM micrograph of MWCNTs after sonication (the Baytube CNT agglomerates can be dispersed in this way) in ethanol is shown in Figure 1. The effective utilization of MWCNTs in composite applications strongly depends on this ability to disperse and distribute homogeneously throughout the matrix. To analyze the state of the dispersion of the filler in the polymer matrix, TEM micrographs were taken for the composites (Figure 2). Even if the shown images are just snapshots of a very low part of the composites, analysis reveals well-dispersed individual nanotubes in the epoxy matrix for all the composites. To some extent, slight agglomeration was observed for 0.37 wt % MWCNTs composite. From the SEM micrographs of the fracture surface after K_{IC} test of the composites (Figure 3), we observe coexistence of small areas with and without MWNTs; however, in the areas with MWCNTs, fine dispersion of nanotubes are observed.

Kinetics of Curing

Figure 4 shows differential scanning calorimetry thermograms during the curing of composites as obtained during first heating

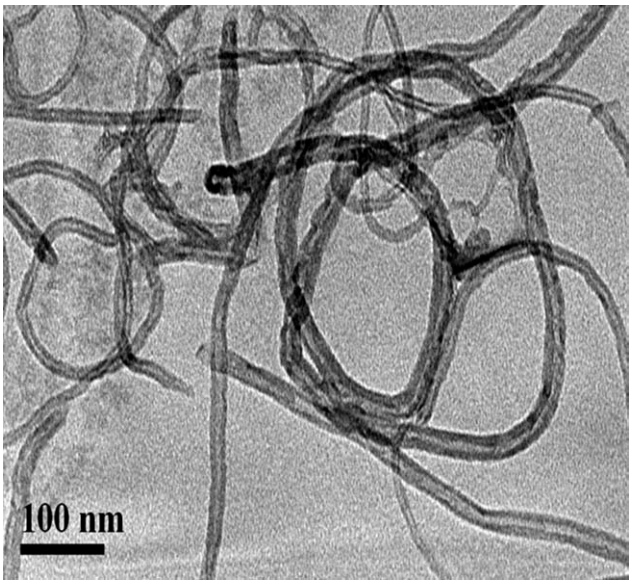

Figure 1. TEM micrograph of MWCNTs used.

in modulated DSC scan. For any given specimen only one exothermic peak was observed due to the polymerization of the DGEBA/amine owing to the heat evolved when epoxide rings are opened during their reaction with amine functionalities. The peak area under the baseline extrapolated to end of the reaction was used to calculate the total heat of reaction (ΔH). The exothermal peak maximum temperature (T_p), ΔH, ΔH_{corr} (ΔH normalized to the epoxy weight content), and T_g and ΔC_p at T_g during the first and second DSC scans, as a function of the concentration of MWCNTs are reported in Table II. It can be seen that ΔH_{corr} is slightly less for MWCNT/epoxy composite. The decrease in ΔH_{corr} (degree of epoxy amine reaction) may be attributed to the dispersed MWCNTs that can hamper the mobility of monomers and lower mobility of monomers may decrease the degree of the reaction.[30,31] The slightly lower T_g of the cured composite compared with the neat resin supports this assumption. It is important to add that, we observe 93 and 90% conversion respectively for neat epoxy resin and 0.37 wt % MWCNT/epoxy composites (Figure 5) during the isothermal DSC runs at 180°C (heating rate 100°C/min to the curing temperature, Perkin-Elmer, Diamond DSC). Again, a reduction in conversion was noticed.

Pressure Volume Temperature Studies

A typical isothermal curing of MWCNTs/thermoset based composites is accompanied by the polymerization shrinkage and vitrification of the thermoset-rich phase. The material shrinkage that occurs during curing can adversely affect the desired tolerance of the final product and hence a PVT study is necessary for thermosetting composites. Figure 6 gives the change in specific volume (V_{sp}) data obtained for neat epoxy/DDS and the epoxy/DDS mixtures containing 0.37 wt % MWCNTs with respect to cure time. A sharp decrease in V_{sp} was observed for both neat epoxy and epoxy composite due to the in-situ epoxy-amine reaction (volume shrinkage).[32] After heating for 2 h, V_{sp} reached an almost constant value for composites, while shrinkage period for the neat epoxy was slightly longer (ca. 2.3 h). The beginning of the plateau region, which was stable up to 13 h, corresponds to the end of the curing reaction.

Dynamic Mechanical Analysis

DMA is a common and valuable technique to characterize the ability of a material to store and dissipate mechanical energy when subjected to deformation in a wide temperature range. Figure 7 illustrates log storage modulus (log E') against temperature for neat epoxy and MWCNT/epoxy composites. Log E' curve demonstrate the load bearing capacity and the stiffness of the sample. The rigid MWCNTs improved the stiffness of the epoxy matrix composites and hence the load bearing capacity of the MWCNT/epoxy composites. The slight increase in the modulus is due to the reinforcement imparted by the MWCNTs, allowing stress transfer from matrix to stronger MWCNTs. There is an inflection point at around 190°C, which indicates the transition from the solid state to the rubbery state, the so-called glass transition temperature (T_g). The T_g values are in agreement with DSC results (Table II). Above the T_g modulus decreases sharply due to the segmental mobility of the polymer chains.

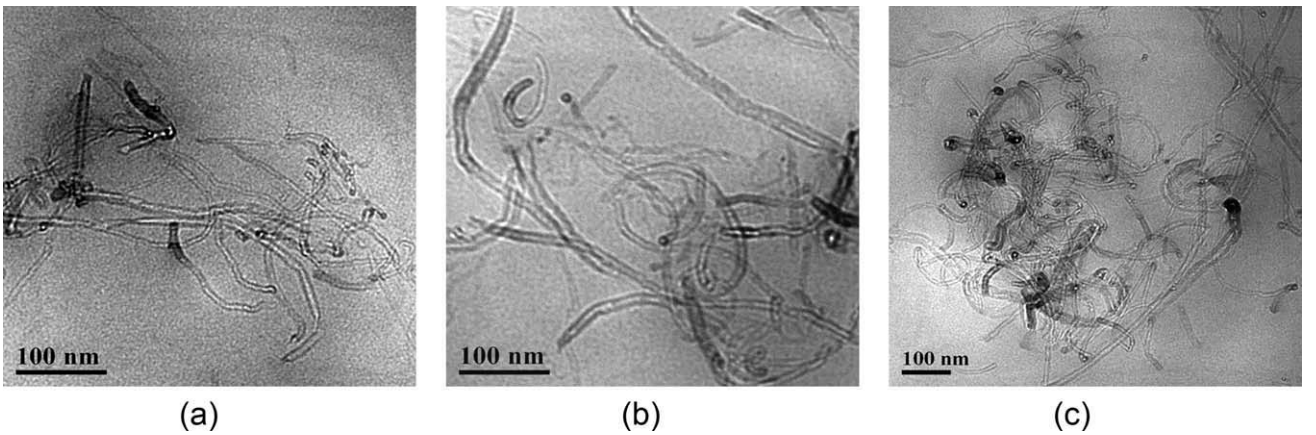

Figure 2. TEM micrographs of MWCNT/epoxy composites; (a) 0.07 wt % MWCNTs, (b) 0.22 wt % MWCNTs, (c) 0.37 wt % MWCNTs.

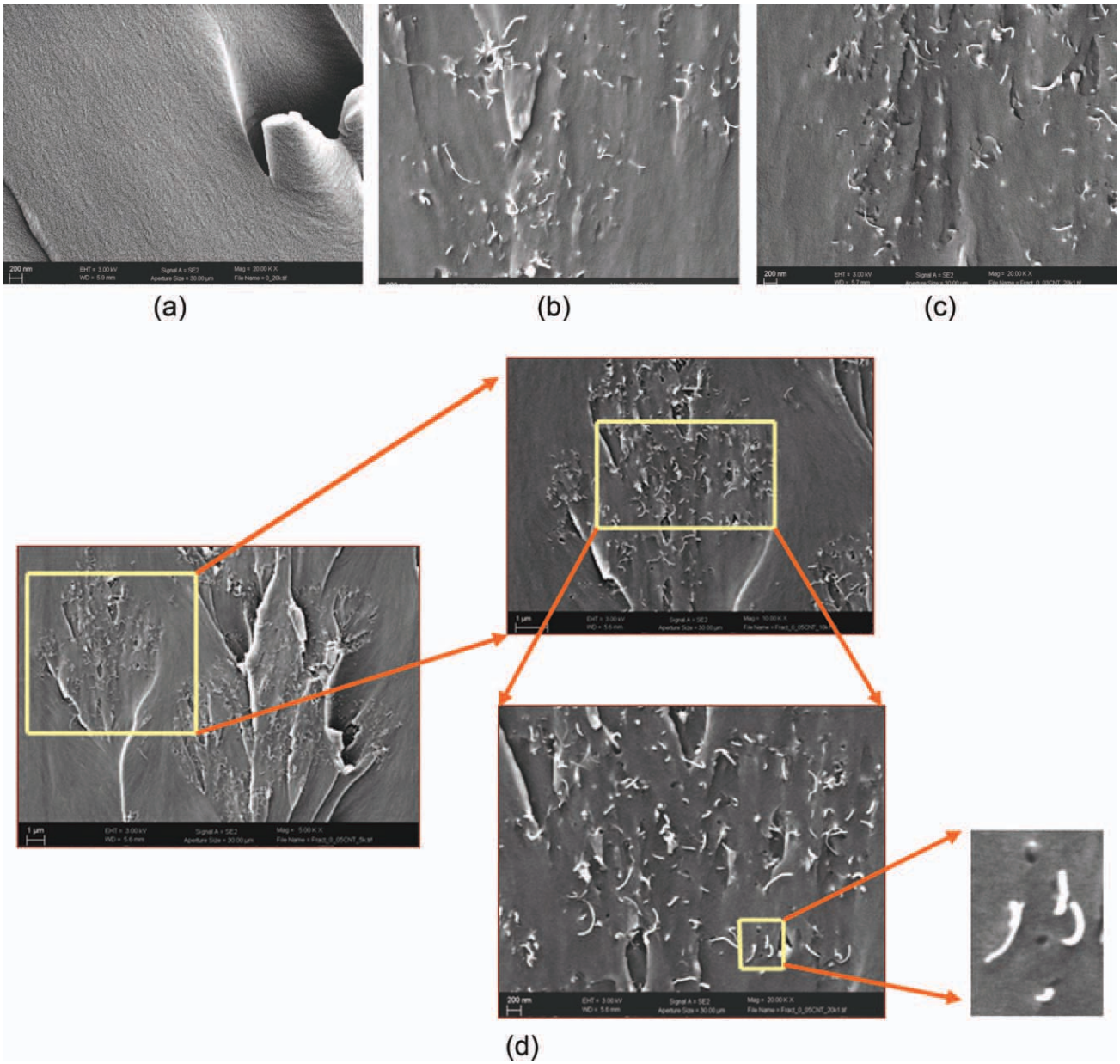

Figure 3. FESEM micrographs of failed surfaces of MWCNT/epoxy composites; (a) neat epoxy, (b) 0.07 wt % MWCNTs, (c) 0.22 wt % MWCNTs, (d) 0.37 wt % MWCNTs. [Color figure can be viewed in the online issue, which is available at wileyonlinelibrary.com.]

Thermomechanical Analysis

Thermal expansion behavior was measured using TMA to investigate the effect of MWCNTs on the dimensional change of the epoxy composite samples. The TMA thermograms of cured epoxy composites are shown in Figure 8. From the thermograms the dimensional change increases with increase in temperature. As expected the response of the neat epoxy sample is greater than MWCNT/epoxy composites. The change in dimension can be explained by the concept of molecule interaction. With increase in temperature molecular vibration increases which causes an increase in the intermolecular distance. However, higher restriction effect in mobilization of MWCNT/epoxy molecules limits the amplitude of vibration especially at high temperatures (between 80 and 180°C). This means that the intermolecular distance in MWCNT/epoxy composites is less compared with that of the epoxy system or, in other words, MWCNTs retard thermal expansion of the molecules up on heating. During heating the composites expand and then undergoes a glassy-to-rubbery transformation (T_g); it then continues to expand in the rubbery phase with a greater linear expansion coefficient, showing the normal expansion behavior of rubber state. The observed drop in the dimension change near to T_g is due to relaxation of below T_g frozen nonequilibrium states of the cured samples. Above T_g the dimension change may be falsified by penetration of the sensor tip into the softened resin, so that a quantification is not meaningful.

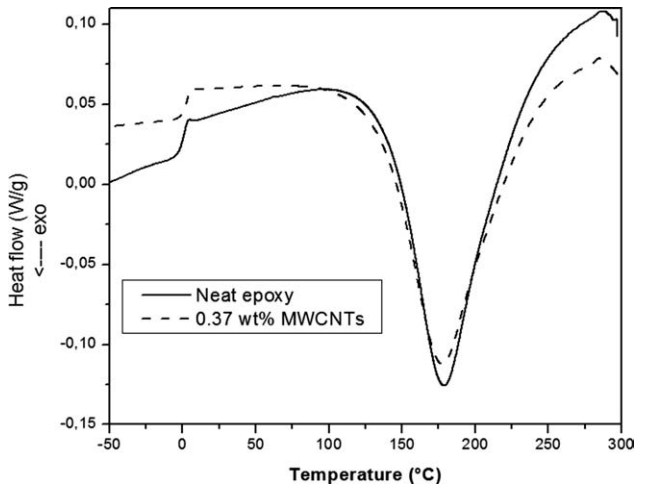

Figure 4. Variation of heat flow with respect to temperature for the pure epoxy and a MWCNT/epoxy composite.

Electrical Properties

The electrical properties of the prepared samples were studied by employing dielectric relaxation spectroscopy. Figure 9 shows the frequency (f) dependence of the real part of the complex electrical conductivity, $\sigma'(f)$, at room temperature for the pure epoxy and the composites containing various amounts of MWCNTs. Depending on the nanotubes concentration, two distinct behaviors can be observed: Electrical ac conductivity increases linearly as frequency increases for the composites with 0.007 and 0.019 wt % MWCNTs as well as for neat epoxy, a typical behavior for insulating materials. Contrarily, the samples with loadings of at least 0.037 wt % MWCNTs exhibit a direct current (d_c) plateau, where σ' is independent of frequency below a critical frequency (f_c). As the amount of MWCNTs increases f_c shifts to higher frequencies and the dc plateau becomes wider. It is clearly seen that the transition from insulating to conducting phase takes place between 0.019 and 0.037 wt % of MWCNTs. Thus, the percolation threshold (p_c), being the critical composition of conducting inclusions where the first network is formed, is located between these two values.

Mechanical Tests

The impact strength of a material describes the energy required to break the specimen under sudden load. The magnitude of the impact strength reflects the ability of the material to resist impact. The Charpy impact tests were carried and impact strengths of epoxy composites were shown in Figure 10. All MWCNT/epoxy composites have significantly higher impact strength compared with the neat crosslinked epoxy. On the other hand, for 0.37 wt % MWCNTs the impact strength decreases, possibly due to nonuniform dispersion of MWCNTs in the epoxy matrix. A maximum of 18% increase in impact energy was achieved at 0.22 wt % MWCNTs.

Fracture toughness is the resistance of material to crack initiation and propagation. It can be seen that fracture toughness of the epoxy resin was improved by the addition of MWCNTs. Plots of the critical-stress-intensity factor (K_{IC}) against concentration of MWCNTs in the cured epoxy are shown in Figure 11. From the experimental observation, a maximum increase of about 38 % in K_{IC} was observed for the 0.22 wt % MWCNTs containing epoxy composite with respect to the neat material. The toughening mechanism is elaborated in the discussion part.

DISCUSSION

From Table II, the first dynamic DSC run shifts the T_gs of the neat epoxy and composites to higher temperature, giving a clear trend to lower T_gs with MWCNTs contents. The increase in the epoxy T_g after the first dynamic DSC scans is due to the crosslinking reaction between epoxy monomer and amine. Dynamic curing induces vitrification, this can be seen from the change in heat capacity (ΔC_p) at T_g, which decreases after the first dynamic DSC scans due to the loss in the number of molecules that can become mobile, due to tight crosslinks.

Pressure–volume–temperature characterization is a well-known tool for the investigation of changes in specific volume with respect to cure time for epoxy systems. From the specific volume value, the percentage volume shrinkage (ΔV_{sp}) of the composites at any time t can be calculated as

$$\Delta V_{sp} = \left(\left(V_{sp,T0} - V_{sp,E}\right)/V_{sp,T0}\right) \times 100 \quad (5)$$

where $V_{sp,T0}$ is the theoretical specific volume of the composites at time $t = 0$ and $V_{sp,E}$ is the experimental specific volume for the composites at any time t. Since MWCNT do not change there structure, the measured volume shrinkage of the composites is always the shrinkage of the epoxy phase. Figure 12(a) reveals a decrease in volume shrinkage by the addition of MWCNTs. Because of the high surface to volume ratio of MWCNTs, some of the epoxy oligomers/polymer chains may generate a constrained polymer layers around the filler surface, which does not undergo shrinkage due to the stabilizing effect of rigid MWCNTs. More over, the physical hindrance of epoxy

Table II. Thermal Properties of Neat Epoxy and MWCNT/Epoxy Composites

Samples	$T_{g\ 1(1st\ heating)}$ (°C)	$\Delta C_{p\ 1(1st\ heating)}$ (J/g K)	$T_{g\ 1(2nd\ heating)}$ (°C)	$\Delta C_{p\ 1(2nd\ heating)}$ (J/g K)	ΔH (J/g$_{(blends)}$ (1st heating)	$\Delta H_{(0,corr)}$ (J/g$_{(epoxy)}$) (1st heating)	T_p (°C) (1st heating)
Neat epoxy	3.7	0.54	195.2	0.24	−394.4	−394.4	179
0.37 wt % MWCNTs	3.6	0.53	191.7	0.26	−385.6	−387.0	178

$T_{g\ 1(1st\ heating)}$, $\Delta C_{p\ 1(1st\ heating)}$, and $T_{g\ 1(2nd\ heating)}$, $\Delta C_{p\ 1(2nd\ heating)}$ are the glass transition temperatures and change in heat capacity at the glass transition (T_g) detected by first and second DSC run. ΔH and $\Delta H_{(0,corr)}$ are the heat of reaction and heat of reaction normalized to the epoxy content for the uncured samples. T_p is the peak maximum temperature of the exothermic curing peak.

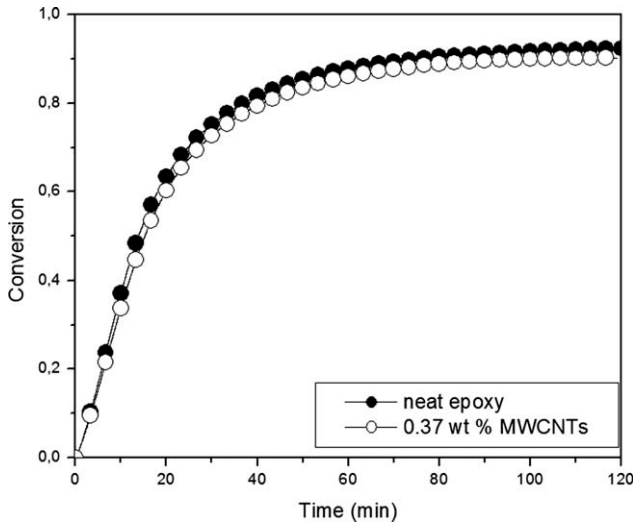

Figure 5. Isothermal DSC curves for the pure epoxy and MWCNT/epoxy composites.

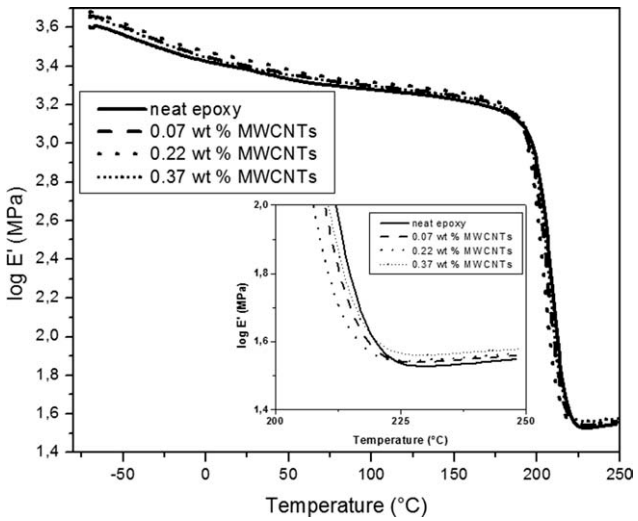

Figure 7. Mechanical characteristics of neat epoxy/DDS and MWCNT/epoxy composites; log E' vs. temperature.

oligomer/polymer chains by individual MWCNTs hamper the curing reaction resulting in a decrease of relative volume shrinkage.[31] In other words, the specific volume change under isothermal and isobaric conditions reflects the internal structure and interactions in the epoxy systems.

Furthermore, we have calculated the normalized shrinkage ($\Delta V_{sp,N}$) with respect to the epoxy volume content in the composite using the equation

$$\Delta V_{sp,N} = \left((\Delta V_{sp})/\text{wt}\,\%\,\text{of epoxy phase}\right) \times 100 \qquad (6)$$

Figure 12(b) shows normalized shrinkage value as a function of the concentration of the MWCNTs. In addition, the normalized shrinkage shows a lower shrinkage for MWCNT/epoxy composites with respect to neat epoxy, i.e., around 10% reduction in normalized shrinkage by the addition of only 0.37 wt% MWCNTs in epoxy resin. These results suggest that the addition of only a small amount of MWCNTs in epoxy matrix can reduce the shrinkage of epoxy matrix by 10%, which is favorable for many epoxy applications.

Curing Kinetics of MWCNT/Epoxy Composites

In view of the PVT data a general equation of state for the specific volume (V_{sp}) dependence on temperature (T) pressure (P) and conversion (X) for epoxy polymerization can be expressed as[33]

$$dV_{sp}/V_{sp} = 1/V_{sp}(dV_{sp}/dT)_{P,X}dT + 1/V_{sp}(dV_{sp}/dX)_{PT}dX + 1/V_{sp}(dV_{sp}/dP)_{T,X}dP \qquad (7)$$

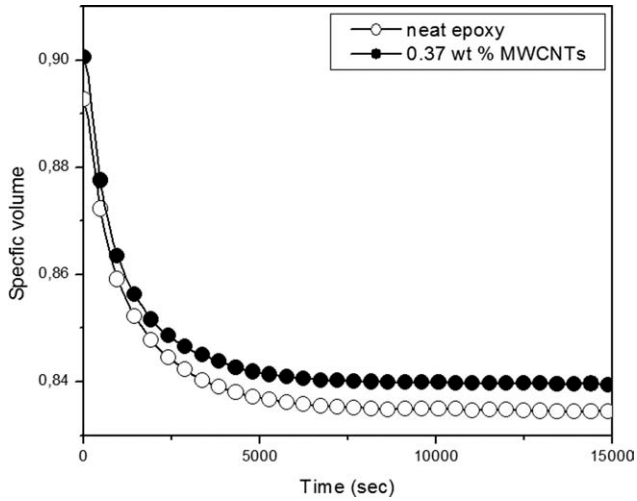

Figure 6. PVT analysis of the epoxy/DDS curing process at 180°C under a pressure of 10 MPa of neat epoxy/DDS mixture and neat epoxy/DDS mixture with 0.37 wt % MWCNTs.

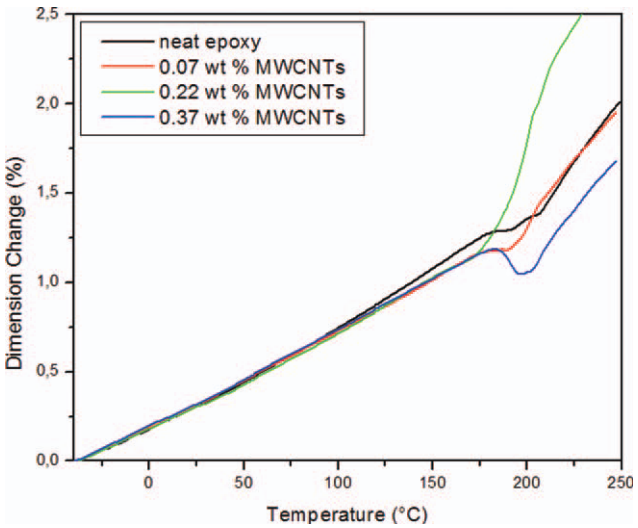

Figure 8. Dimensional change vs. temperature for MWCNT/epoxy composites. [Color figure can be viewed in the online issue, which is available at wileyonlinelibrary.com.]

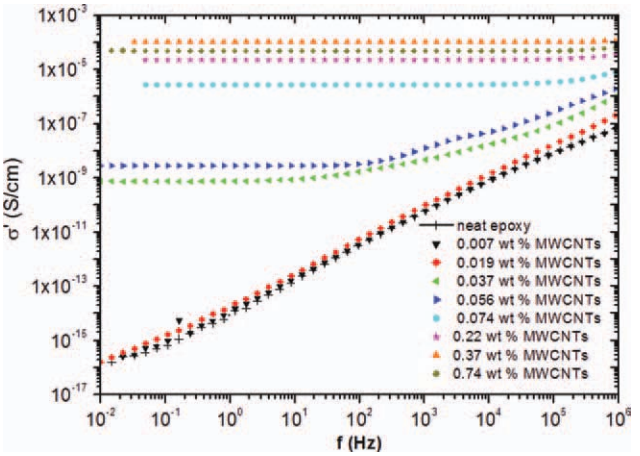

Figure 9. Frequency (f) dependence of the real part of the complex electrical conductivity, σ' at room temperature for the pure epoxy and the composites containing various amounts of MWCNTs. [Color figure can be viewed in the online issue, which is available at wileyonlinelibrary.com.]

For curing at constant T and P the volume changes between the times 0 to t can be given by Eq. (8).

$$\int_0^t dV_{sp} = \int_0^x dV_{sp,t} R_{(XTP)} dX \tag{8}$$

where $R_{(XTP)=}\ 1/V_{sp}\ (dV_{sp}/dX)_{PT}$ is the volumetric coefficient associated with polymerization.

For neat systems, their exist a linear relationship between epoxy conversion and epoxide cure shrinkage and then the conversion of the composites X_{comp} could be represented as[34,35]

$$X_{comp} = \left((\Delta V_{sp,N\,comp})/(\Delta V_{sp,epoxide(t\to\infty)})\right) \times 100 \tag{9}$$

The conversion obtained from the PVT measurements for neat epoxy and with 0.37 wt % MWCNTs modified epoxy are shown in Figure 12(c). The final conversion value from the plot (the plot shows only up to 15,000 s, but the run lasted 13 h) are 100 and 90% for neat epoxy and for the MWCNT/epoxy composites, respectively. In this context 100% conversion means the maximum possible conversion of epoxy units under the chosen curing conditions. We are aware that 100% chemical conversion of epoxy and amino groups in an epoxy resin are hardly possible due to vitrification. However, from the figure it becomes clear that the final epoxy conversion decreases with addition of MWCNTs. The difference of 10% in shrinkage is not caused only by the reduced conversion but it overlaps with the stabilizing effect of the MWCNTs on the epoxy materials in the constrained layers surrounding the MWCNTs, which will shrink less during curing than the pure epoxy phase. From DSC measurements, a reduction in conversion of <5% due to MWCNTs can be evaluated. The reduced shrinkage of 10% measured by PVT must be therefore caused by the reduced epoxy/amine conversion in combination with the stability effect of MWCNTs against the shrinkage deformation of the constrained epoxy layer.

The dynamic mechanical analysis also supports PVT and DSC results. As mentioned in section 4.4, there is a prominent increase in the modulus of the matrix with the incorporation of MWCNTs in the glassy state. Similarly, the modulus of the composites is higher in the rubbery state (Figure 7), which clearly indicates the reinforcing effect of MWCNTs supporting the assumption of a stabilizing effect of MWCNTs against shrinkage deformation of the constrained epoxy layer.[36]

Loss modulus is a measure of energy dissipation and can be used to analyze the viscous response of the material. The loss modulus increases with MWCNTs content [Figure 13(a)]. The dispersed MWCNTs dissipate energy due to resistance against viscoelastic deformation of the surrounding epoxy matrix.[37] The main peak at around 210°C corresponds to the T_g of the crosslinked epoxy phase and a shoulder at around 160°C indicates the presence of a lower temperature glass transition, beside the main transition at the same temperature as the crosslinked neat

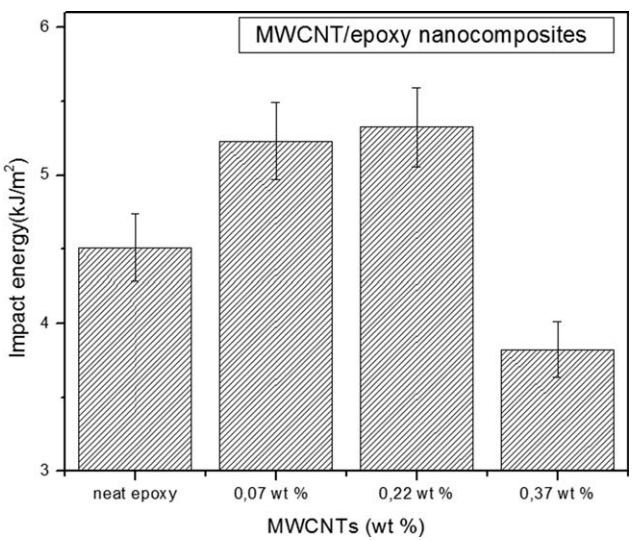

Figure 10. Impact strength of MWCNT/epoxy composites.

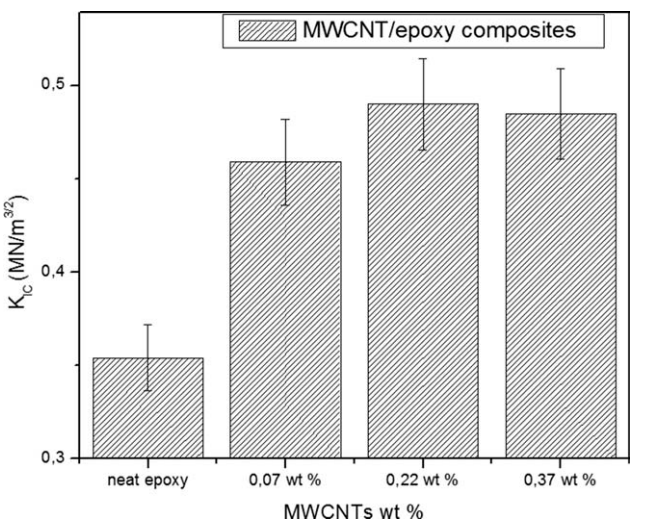

Figure 11. Fracture toughness of MWCNT/epoxy composites.

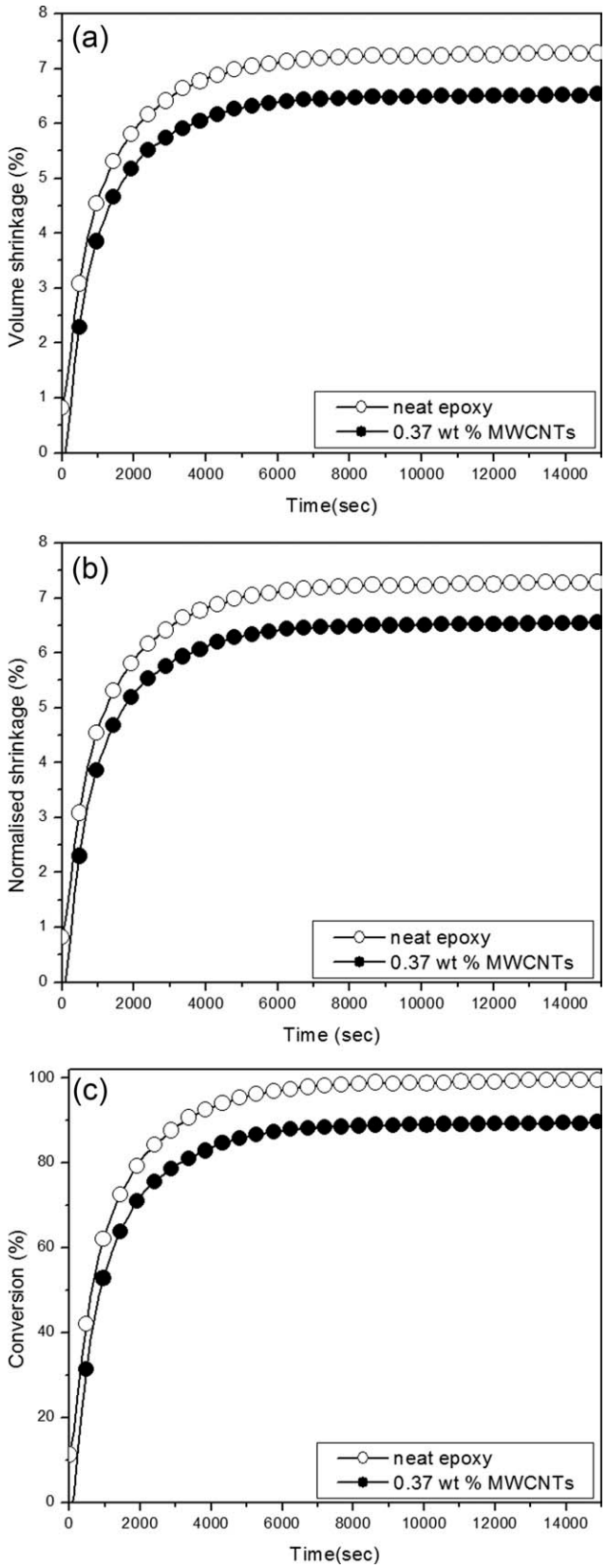

Figure 12. PVT analysis of the epoxy/DDS curing process at 180°C under a pressure of 10 MPa: (a) volume shrinkage vs. curing time, (b) normalized shrinkage vs. curing time, (c) Conversion vs. curing time.

epoxy resin. This suggests the presence of a fraction of IPN type structure consisting of epoxy polymers with higher mobility due to a different degree of crosslinking. Careful examination of loss modulus curves reveals a soft peak at around 60°C, which may be the ω-relaxation peak of the lower crosslink density sites in the epoxy network or the β-relaxation overtones of the regions of higher crosslink density, which are occluded in the lower crosslink density matrix.[38]

The ratio of loss modulus to storage modulus is measured as tan δ. The tan δ against temperature plots are given in Figure 13(b). For neat epoxy and epoxy composites, there exists a well-defined relaxation peak centered at 200°C which is ascribed to the glass transition temperature (T_g) of the cured epoxy monomer. The tan δ peak heights, peak widths at half-height, and peak areas are summarized in Table III. It is important to mention that the parameters obtained from tan δ profile are comparable for all the systems studied, except the small reduction in T_g of the composites.

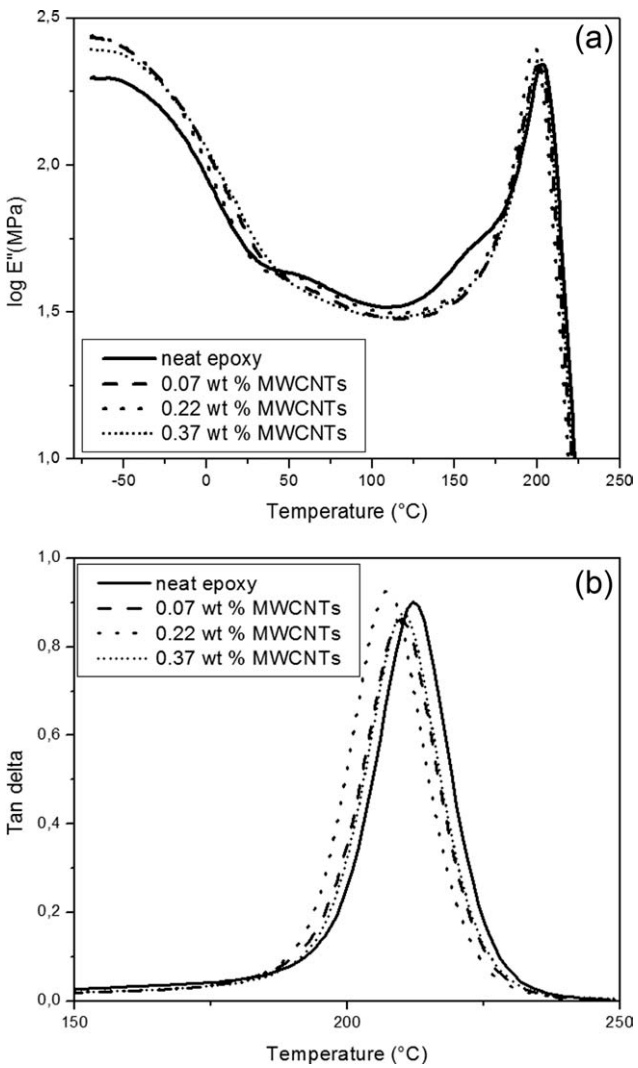

Figure 13. Mechanical characteristics of neat epoxy/DDS and MWCNT/epoxy composites; (a) log E" vs. temperature, (b) tan δ vs. temperature.

Table III. Parameters Obtained from tan δ Profile

Samples	tan δ peak height	tan δ peak width at half height	tan δ peak area	tan δ peak °C	M_c (g/mol)	$\upsilon_e \times 10^{27}$ chains/m^3
Neat epoxy	0.89	16	17.88	212	322.31	2.24
0.07 wt % MWCNTs	0.86	17	16.91	210	327.73	2.20
0.22 wt % MWCNTs	0.92	17	17.82	207	336.21	2.14
0.37 wt % MWCNTs	0.86	16	16.13	210	327.73	2.20

The molecular weight between the crosslinks (M_c), which is an indirect measure of crosslink density of epoxy resin, can be calculated from the T_g of epoxy rich phase using the Eq. (10).[39]

$$M_c = \frac{3.9 \times 10^4}{T_g - T_{g0}} \tag{10}$$

where T_g is the glass transition temperature of the crosslinked epoxy resin and T_{g0} is the glass transition temperature of uncrosslinked polymer having same composition as crosslinked polymer. The value of T_{g0} was taken as 91°C for DGEBA/DDS system.[40] The effective crosslink density (υ_e) was calculated from M_c using the Eq. (11).[39]

$$\upsilon_e = \frac{\rho N_A}{M_c} \tag{11}$$

where ρ is the density and N_A is Avogadro's number.

The molecular weight between the crosslinks (M_c) and the effective crosslink density (υ_e) are summarized in Table III. The increase in M_c and consequent decrease in crosslink density is evident from the table again proving reduced epoxy/amine reaction in MWCNTs-containing composites.

Important factors that influence the mechanical properties (fracture toughness) include the morphology of the composites, the amount of modifier, the dispersion of the nanotubes, the interfacial adhesion, and the curing conditions. Roughness of the fracture surface is also crucial for getting improved fracture toughness. Figure 3 reveals the SEM micrographs of samples observed under microscope after the K_{IC} fracture test. SEM fracture micrographs after impact fracture were similar to fracture micrographs of the fractured samples after fracture mechanics test and hence were not given in the manuscript. Figure 3(a) shows the SEM micrograph of the neat epoxy system, which reveals a single phase. The fracture surface was typically rather flat and smooth, indicating the typical brittle nature of the material. Compared with the smooth fracture surface of the neat epoxy, the fracture surface of the MWCNT/epoxy-composites, [Figure 3(b–d)], are significantly rougher.[25] As mentioned in Section 4.1, we observe coexistence of small areas with and without MWCNTs; however, in the areas with MWCNTs fine dispersion of nanotubes is observed. It is important to mention that in the region outside the nanotubes, the fracture surface is quite smooth, similar to neat epoxy. On the other hand, fracture surface with MWCNTs are rough, these features show that the nanotubes interact with the crack path and result in crack deflection and a more tortuous fracture path, or in other words the carbon nanotubes can effectively interact with the crack front and this is the likely one of the reason why the nanocomposites show enhanced fracture toughness.[15] The fracture surface reveals that the nanotubes are still partially embedded in the matrix and pull out took place resulting in the observation bare nanotube lengths of >200 nm nanotubes. On the other hand few small cavities around 50 nm are visible on the surface of the crosslinked epoxy, due to the complete pull out of the carbon nanotubes [Figure 3(d)]. The pull out is understandable considering the non-functionalized character of the MWCNTs, indicating poor adhesion between the matrix and MWCNTs.[24,41–43]

From the fracture micrographs, the main toughening mechanism seems to be enhanced surface roughness and fiber pull out. These experimental findings are in agreement with an argument proposed by Wichmann et al.,[43] who stated that nanotube pull-out represents an important source of toughness for composites and propose that the increased toughness is due to energy dissipation from interfacial debonding and fiber pullout of nanotubes.

CONCLUSIONS

The PVT studies revealed that a small amount of MWCNTs in epoxy system can effectively reduce the volume shrinkage of the epoxy phase. We believe that constrained layers around the filler are formed. In these layers, the mobility and therefore the curing reactions are hampered, resulting in a small reduction in crosslink density. Furthermore, in these constrained layers shrinkage during crosslinking is reduced due to the rigid MWCNTs neighborhood. Both effects potentially reduce the epoxy volume shrinkage resulting in better dimension stability, favorable for many epoxy applications. This conclusion related to the limitations of shrinkage due to the nanoparticles, is subject to calorimetric conversion showing the same differences in dynamic and isothermal experiments. The fine dispersion of the MWCNTs in the matrix results in the formation of conductive percolating structures at very small filler contents, exhibiting high electrical conductivity already with 0.037 wt % MWCNTs in the composites. Nanotube pull-out and fracture surface roughness were largely observed in these composites and are considered to be the main source of energy dissipation leading to the improved toughness especially below the percolation concentration.

ACKNOWLEDGMENTS

The companies Bayer Material Science AG (Leverkusen, Germany) and Atul, India are acknowledged for the kind supply of MWCNTs,

epoxy monomer and curing agent. Authors thank Mr. H. Kunath, IPF Dresden, for general technical assistance.

REFERENCES

1. Monthioux, M.; Kuznetsov, V. L. *Carbon* **2006,** *44*, 1621.
2. Zhang, M.; Li, J. *Mater. Today* **2009,** *12*, 12.
3. Thostenson, E. T.; Ren, Z.; Chou, T. W. *Compos. Sci. Technol.* **2001,** *61*, 1899.
4. Inukai, S.; Niihara, K.; Noguchi, T.; Ueki, H.; Magario, A.; Yamada, E.; Inagaki, S.; Endo, M. *Ind. Eng. Chem. Res.* **2011,** *50*, 8016.
5. Ajayan, P. M.; Stephan, O.; Colliex, C.; Trauth, D. *Science* **1994,** *265*, 1212.
6. Logakis, E.; Pandis, C.; Peoglos, V.; Pissis, P.; Pionteck, J.; Pötschke, P.; Micusik, M.; Omastova, M. *Polymer* **2009,** *50*, 5103.
7. Logakis, E.; Pollatos, E.; Pandis, C.; Peoglos, V.; Zuburtikudis, I.; Delides, C. G.; Vatalis, A.; Gjoka, M.; Syskakis, E.; Viras, K.; Pissis, P. *Compos. Sci. Technol.* **2010,** *70*, 328.
8. Spitalsky, Z.; Tasis, D.; Papagelis, K.; Galiotis, C. *Prog. Polym. Sci.* **2010,** *35*, 357.
9. Gojny, F. H.; Schulte, K. *Compos. Sci. Technol.* **2004,** *64*, 2303.
10. Sui, G.; Zhong, W. H.; Liu, M. C.; Wu, P. H. *Mater. Sci. Eng. A* **2009,** *512*, 139.
11. Goodman, S. H. Handbook of Thermoset Plastics, 2nd ed.; Noyes Publications: Westwood, NJ, **1999;** Chapter Epoxy Resins, p 193; doi:10.1016/B978–081551421-3.50009–6.
12. Fink, J. K. Epoxy Resins. Reactive Polymers Fundamentals and Applications; William Andrew: Norwich, NY, **2005;** Chapter 3, p 139; doi:10.1016/B978-081551515-9.50005-6.
13. Hodgkin, J. Thermosets. Encyclopedia of Materials: Science and Technology; Elsevier, Amsterdam, The Netherlands, **2008;** p 9215; 10.1016/B0-08-043152-6/01660–0.
14. Varma, K.; Gupta, V. B. Thermosetting Resin-Properties. Comprehensive Composite Materials; Elsevier Science: Amsterdam, The Netherlands, **2003;** p 1; doi:10.1016/B0–08-042993-9/00177-7.
15. Thostenson, E. T.; Chou, T.-W. *Carbon* **2006,** *44*, 3022.
16. Lau, K.; Gu, C.; Hui, D. *Compos. B* **2006,** *37*, 425.
17. Lau, K.; Shi, S. *Carbon* **2002,** *40*, 2965.
18. Martin, C. A.; Sandler, J. K. W.; Shaffer, M. S. P.; Schwarz, M.-K.; Bauhofer, W.; Schulte, K.; Windle, A. H. *Compos. Sci. Technol.* **2004,** *64*, 2309.
19. Yu, N.; Zhang, Z. H.; He, S. Y. *Mater. Sci. Eng. A* **2008,** *494*, 380.
20. Gojny, F. H.; Wichmann, M. H. G.; Fiedler, B.; Schulte, K. *Compos. Sci. Technol.* **2005,** *65*, 2300.
21. Moisala, Q. L.; Kinloch, I. A.; Windle, A. H. *Compos. Sci. Technol.* **2006,** *66*, 1285.
22. Abdalla, M.; Dean, D.; Robinson, P.; Nyairo, E. *Polymer* **2008,** *49*, 3310.
23. Xie, H.; Liu, B.; Sun, Q.; Yuan, Z.; Shen, J.; Rongshi, C. *J. Appl. Polym. Sci.* **2005,** *96*, 329.
24. Lau, K.; Hui, D. *Carbon* **2002,** *40*, 1605.
25. Hernández-Pérez, A.; Avilés, F.; May-Pat, A.; Valadez-González, A.; Herrera-Franco, P. J.; Bartolo-Pérez, P. *Compos. Sci. Technol.* **2008,** *68*, 1422.
26. Gong, X. Y.; Liu, J.; Baskaran, S.; Voise, R. D.; Young, J. S. *Chem. Mater.* **2000,** *12*, 1049.
27. Allaoui, A.; Bai, S.; Cheng, H. M.; Bai, J. B. *Compos. Sci. Technol.* **2002,** *62*, 1993.
28. Zheng, Y. P.; Zhang, J. X.; Yu, P. Y.; Shi, W.; Wang, B. *Polym.-Plast. Technol. Eng.* **2010,** *49*, 1016.
29. Saxena, A.; Francis, B.; Lakshmana Rao, V.; Ninan, K. N. *J. Appl. Polym. Sci.* **2006,** *100*, 3536.
30. Tao, K.; Yang, S.; Grunlan, J. C.; Kim, Y. S.; Dang, B.; Deng, Y. *J. Appl. Polym. Sci.* **2006,** *102*, 5248.
31. Kim, S. H.; Lee, W.; Park, J. M. *Carbon* **2009,** *47*, 2699.
32. Ramos, J. A.; Pagani, N.; Riccardi, C. C.; Borrajo, J.; Goyanes, S. N.; Mondragon, I. *Polymer* **2005,** *46*, 3323.
33. Boyard, N.; Vayer, M.; Sinturel, C.; Eree, R.; Delaunay, D. *J. Appl. Polym. Sci.* **2003,** *88*, 1258.
34. Hill, R. R.; Muzumdar, S. V.; Lee, L. *J. Polym. Eng. Sci.* **1995,** *35*, 852.
35. Zarrelli, M.; Skordos, A. A.; Patridge, I. K. *Plast. Rubber Compos.* **2002,** *31*, 377.
36. N.Hameed, P. A.; Sreekumar, B.; Francis, W.; Yang, S. T. *Compos: Part A* **2007,** *38*, 2422.
37. Montazeri, A.; Montazeri, N. *Mater Des* **2011,** *32*, 2301.
38. Mathew, V. S.; Jyotishkumar, P.; George, S. C.; Gopalakrishnan, P.; Delbreilh, L.; Saiter, J. M.; Saikia, P. J.; Thomas, S. *J. Appl. Polym. Sci.* **2012,** *125*, 804.
39. Nielsen, L. E. *J. Macromol. Sci. Rev. Macromol. Chem.* **1969,** *3*, 69.
40. Bellenger, V.; Verdu, J.; Morel, E. *J. Polym. Sci. Part B Polym. Phys.* **1987,** *25*, 1219.
41. Breton, Y.; Desarmot, G.; Salvetat, J. P.; Delpeux, S.; Sinturel, C.; Beguin, F.; Bonnamy, S. *Carbon* **2004,** *42*, 1027.
42. Song, Y.; Youn, J. R. *Carbon* **2005,** *43*, 1378.
43. Wichmann, M. H. G.; Schulte, K.; Wagner, H. D. *Compos. Sci. Technol.* **2008,** *68*, 329.